

Supplementary material for “Cyclops states in repulsive Kuramoto networks: the role of higher-order coupling”

Vyacheslav O. Munyayev¹, Maxim I. Bolotov¹, Lev A. Smirnov¹, Grigory V. Osipov¹, and Igor Belykh²

¹*Department of Control Theory, Lobachevsky State University of Nizhny Novgorod,
23 Gagarin Avenue, Nizhny Novgorod, 603022, Russia*

²*Department of Mathematics and Statistics and Neuroscience Institute,
Georgia State University, P.O. Box 4110, Atlanta, Georgia, 30302-410, USA*

I. STABILITY CONDITIONS FOR GENERALIZED SPLAY STATES

This part of the Supplementary Material provides the derivation of the stability condition (3) in the main text, related to the system (1) with the first-order coupling ($l=1$). We consider a generalized splay state:

$$\theta_j = \omega t + \varphi_j, \quad \frac{1}{N} \sum_{j=1}^N e^{i\varphi_j} = 0, \quad (\text{S.1})$$

where $\varphi_j \in [0, 2\pi]$, $j = 1, \dots, N$ are constant phases. To study the local stability of (S.1), from (1) with $l = 1$ we derive the variational equations for the evolution of infinitesimal perturbations $\delta\theta_j$:

$$m\delta\ddot{\theta}_j + \delta\dot{\theta}_j = \frac{1}{N} \sum_{k=1}^N \cos(\Delta_{jk} + \alpha) \delta\theta_k, \quad (\text{S.2})$$

where $\Delta_{jk} = \varphi_j - \varphi_k$. We seek solutions of the linear system (S.2) with constant coefficients in the form $\delta\theta_j = a_j e^{\lambda t}$. This yields a system of algebraic equations:

$$ba_j + \sum_{k=1}^N a_k \cos(\Delta_{jk} + \alpha) = 0, \quad j = 1, \dots, N, \quad (\text{S.3})$$

where $b = -N\lambda(m\lambda + 1)$. System (S.3) has a nontrivial solution if its determinant

$$A(b) = \begin{vmatrix} b + \cos \alpha & \cos(\Delta_{12} + \alpha) & \cos(\Delta_{13} + \alpha) & \dots & \cos(\Delta_{1N} + \alpha) \\ \cos(\Delta_{21} + \alpha) & b + \cos \alpha & \cos(\Delta_{23} + \alpha) & \dots & \cos(\Delta_{2N} + \alpha) \\ \cos(\Delta_{31} + \alpha) & \cos(\Delta_{32} + \alpha) & b + \cos \alpha & \dots & \cos(\Delta_{3N} + \alpha) \\ \vdots & \vdots & \vdots & \ddots & \vdots \\ \cos(\Delta_{N1} + \alpha) & \cos(\Delta_{N2} + \alpha) & \cos(\Delta_{N3} + \alpha) & \dots & b + \cos \alpha \end{vmatrix} = 0. \quad (\text{S.4})$$

To simplify the analysis of (S.4), we introduce the matrices

$$M(j_1, j_2, \dots, j_n) = \begin{pmatrix} \cos(\Delta_{j_1 j_1} + \alpha) & \cos(\Delta_{j_1 j_2} + \alpha) & \dots & \cos(\Delta_{j_1 j_n} + \alpha) \\ \cos(\Delta_{j_2 j_1} + \alpha) & \cos(\Delta_{j_2 j_2} + \alpha) & \dots & \cos(\Delta_{j_2 j_n} + \alpha) \\ \vdots & \vdots & \ddots & \vdots \\ \cos(\Delta_{j_n j_1} + \alpha) & \cos(\Delta_{j_n j_2} + \alpha) & \dots & \cos(\Delta_{j_n j_n} + \alpha) \end{pmatrix}. \quad (\text{S.5})$$

It is straightforward to show that

$|M(j_1, j_2, \dots, j_n)| = 0$ for $n \geq 3$. In fact, any matrix $M(j_1, j_2, \dots, j_n)$ may be written as the sum of two matrices with rank 1: $M = \frac{1}{2} e^{i\alpha} v v^\dagger + c.c.$, where the vector $v = (e^{i\varphi_{j_1}}, e^{i\varphi_{j_2}}, \dots, e^{i\varphi_{j_n}})^T$, $\text{rank}(v v^\dagger) = 1$. Therefore, $\text{rank}(M) \leq 2$ yielding the zero determinant of M .

Taking into account that $A(b) = |xI + M(1, 2, \dots, N)|$, we obtain

$$A(b) = b^{N-2} \left(b^2 + N \cos \alpha b \sum_{j < k} |M(j, k)| \right). \quad (\text{S.6})$$

Note that $|M(j, k)| = \sin^2(\Delta_{jk})$, and therefore $\sum_{j < k} |M(j, k)| = \frac{N^2}{4} (1 - |R_2|^2)$, where R_2 is the second moment of the Kuramoto order parameter: $R_2 = \frac{1}{N} \sum_{k=1}^N e^{2i\varphi_k}$. Thus, we obtain

$$A(x) = b^{N-2} \left[b^2 + N \cos \alpha b + \frac{N^2}{4} (1 - |R_2|^2) \right]. \quad (\text{S.7})$$

We can now find all eigenvalues λ . There are $N - 2$ zero eigenvalues and $N - 2$ with $\lambda = -1/m$. The other four eigenvalues can be found from the characteristic equation:

$$\lambda^4 + \frac{2}{m} \lambda^3 + \frac{1}{m} \left(\frac{1}{m} - \cos \alpha \right) \lambda^2 - \frac{\cos \alpha}{m^2} \lambda + \frac{1}{4m^2} (1 - |R_2|^2) = 0. \quad (\text{S.8})$$

so that

$$\lambda_{1,2,3,4} = -\frac{1}{2m} \left(1 \pm \sqrt{1 + 2m \left(\cos \alpha \pm \sqrt{|R_2|^2 - \sin^2 \alpha} \right)} \right). \quad (\text{S.9})$$

The criterion (S.9) is identical, up to a parameter re-scaling, to the one given in Corollary 9 in Berner et al., *Chaos*, 31, 073128 (2021) (Reference [47] in the main text).

To make the stability criterion more explicit and manageable, we prefer to use the Routh-Hurwitz stability criterion to (S.8) by considering the corresponding Hurwitz matrix

$$H = \begin{pmatrix} \frac{2}{m} & -\frac{\cos \alpha}{m^2} & 0 & 0 \\ 1 & \frac{1}{m} \left(\frac{1}{m} - \cos \alpha \right) & \frac{1}{4m^2} (1 - |R_2|^2) & 0 \\ 0 & \frac{2}{m} & -\frac{\cos \alpha}{m^2} & 0 \\ 0 & 1 & \frac{1}{m} \left(\frac{1}{m} - \cos \alpha \right) & \frac{1}{4m^2} (1 - |R_2|^2) \end{pmatrix}. \quad (\text{S.10})$$

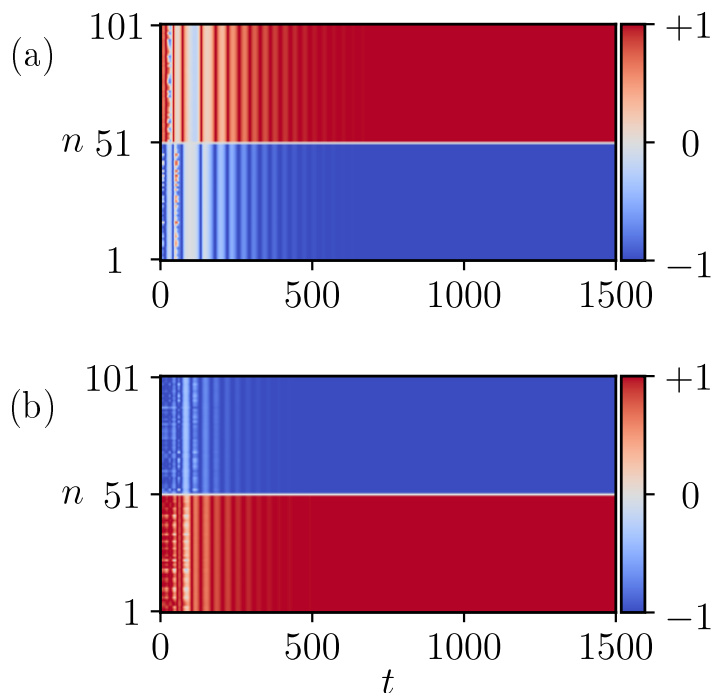
By the Routh-Hurwitz stability criterion, the variational equations (S.2) are stable if

$$\frac{2}{m} - \cos \alpha > 0, \quad |R_2|^2 - 1 - \cos \alpha \left(\frac{2}{m} - \cos \alpha \right) > 0. \quad (\text{S.11})$$

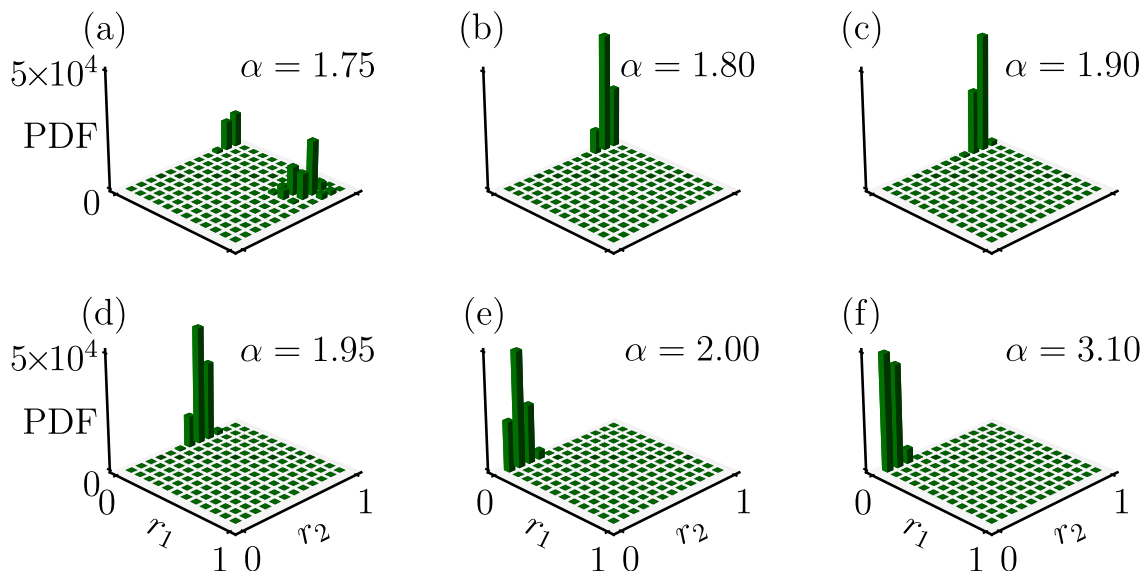
The first inequality is always fulfilled, given $m > 0$ and the considered range of repulsive coupling $\alpha \in (\pi/2, \pi)$. The second equality yields the condition (3) in the main text (with $|R_2| \equiv r_2$). This completes the proof.

II. CYCLOPS STATES IN NETWORKS WITH $N = 101$

This part of the Supplementary Material provides evidence that symmetric cyclops states are the prevalent states in large networks (1).

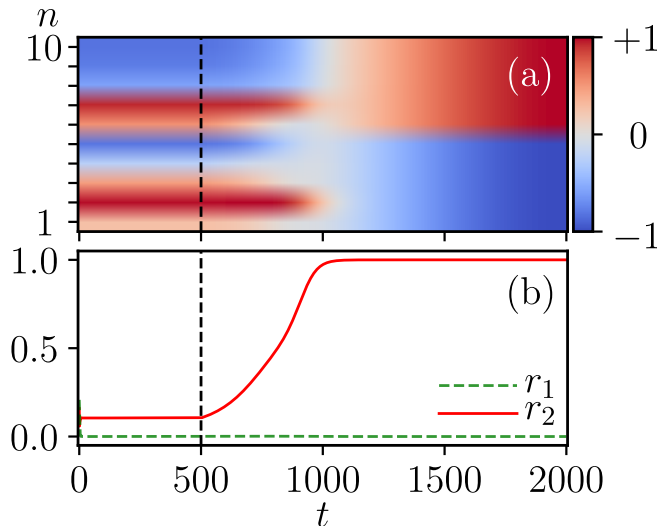


Supplementary Figure 1: (a) The onset of a stable cyclops state in the system (1) for $N = 101$, $m = 1.0$, $\omega = 1.0$, $\alpha = 1.6$. (b) Cyclops state in the system (1) with second harmonic for $N = 101$, $m = 1.0$, $\alpha = 1.6$, $\varepsilon_2 = 0.01$, $\alpha_2 = 0.1$. Colors indicate the sines of phase differences, $\sin(\theta_n(t) - \theta_{51}(t))$. The initial conditions are chosen in the form of a randomly perturbed cyclops state (addition to the phases is a uniformly distributed random variable on a segment $[-0.5, 0.5]$).



Supplementary Figure 2: Histograms for a numerically calculated PDF of the (r_1, r_2) distribution for $N = 101$, $m = 1.0$, $\omega = 1.0$, $K_2 = 0$, $K_3 = 0$ and $\alpha = 1.75$ (a), $\alpha = 1.80$ (b), $\alpha = 1.90$ (c), $\alpha = 1.95$ (d), $\alpha = 2.00$ (e), $\alpha = 3.10$ (f). Cyclops states with a maximum r_2 are the prevalent rhythms in (b), (c), and (d).

III. THE ADDITION OF THE SECOND HARMONICS INDUCES A STABLE TWO-CLUSTER STATE IN THE NETWORK WITH $N = 10$



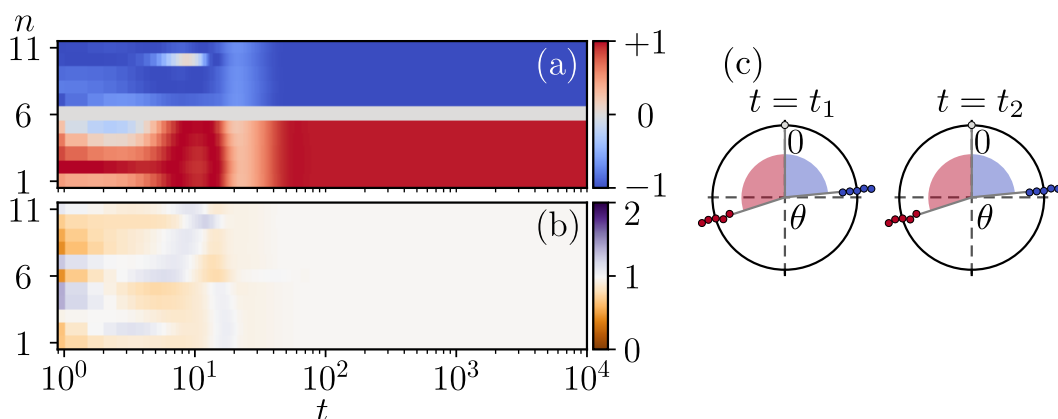
Supplementary Figure 3: The role of the second harmonic in stabilizing a two-cluster state in the system (1) with $N = 10$, $m = 1.0$, $\omega = 1.7$, $\alpha = 3.1$. The system with only the first-order coupling ($K_2 = 0$) evolves into a generalized splay state with $r_1 = 0$ from random initial conditions for $0 < t < 500$. Switching on the second harmonic with $K_2 = 0.008$ and $\alpha_2 = 0.2$ induces a stable two-cluster state ($500 < t < 2000$). (a) Colors indicate $\sin(\theta_n(t) - \omega t)$. (b) The corresponding values of r_1 and r_2 .

IV. CYCLOPS STATES IN NETWORKS OF NONIDENTICAL OSCILLATORS

Here, we demonstrate that cyclops states are resistant to intrinsic frequency detuning. We consider the system of nonidentical Kuramoto-Sakaguchi phase oscillators with inertia

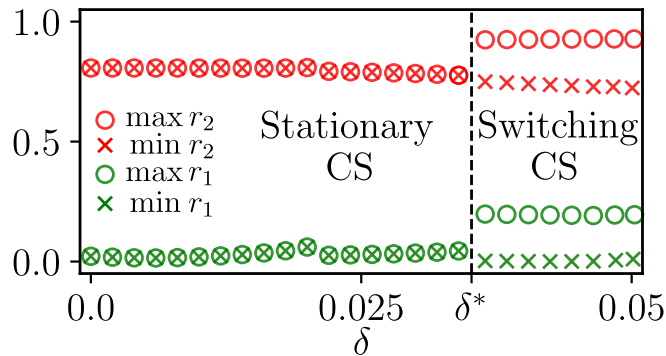
$$m\ddot{\theta}_j + \dot{\theta}_j = \omega_j + \frac{1}{N} \sum_{k=1}^N \sum_{q=1}^l K_q \sin[q(\theta_k - \theta_j) - \alpha_q], \quad (\text{S.12})$$

where intrinsic frequencies ω_n are uniformly distributed random variables on the interval $[\Omega_1, \Omega_2]$. This system is identical to the original system (1) except for the frequency mismatch. As demonstrated in Supplementary Fig. 4, cyclops states emerge robustly in the system (S.12) when the coupling function includes both the first and second harmonics. It should be noted that although the phases of the oscillators within each coherent cluster may not perfectly align due to frequency mismatches, they remain relatively close to each other (as seen in Supplementary Fig. 4a,c). Additionally, the instantaneous frequencies of all oscillators are equal (as depicted in Supplementary Fig. 4b).



Supplementary Figure 4: Stable cyclops state in system (S.12) with mismatched frequencies ω_j (evenly distributed over the interval $[\Omega_1, \Omega_2]$) with $\Omega_1 = 0.998$, $\Omega_2 = 1.002$ for $N = 11$, $m = 1.0$, $K_1 = 1$, $\alpha_1 \equiv \alpha = 1.8$, $K_2 = 0.1$, $\alpha_2 = 0.2$. (a) Time series for the sines of the phase differences, $\sin(\theta_j(t) - \theta_6(t))$. (b) Instantaneous frequencies $\dot{\theta}_j(t)$. (c) Phases $\theta_j(t) - \theta_6(t)$ at various time instants ($t_1 = 9000$, $t_2 = 10000$).

Supplementary Figure 5 illustrates the robustness of the cyclops state in the network of Supplementary Figure 4 as a function of frequency detuning δ .



Supplementary Figure 5: Persistence of cyclops states in system (S.12) with mismatched frequencies ω_j distributed evenly over the interval $[\omega - \delta, \omega + \delta]$, where $\omega = 1.7$ and δ is a frequency detuning. Other parameters $N = 11$, $m = 1.0$, $K_1 = 1$, $\alpha_1 \equiv \alpha = 1.8$, $K_2 = 0.1$, $\alpha_2 = 0.2$. Global maxima (circles) and minima (crosses) of order parameter r_1 (green markers) and r_2 (red markers). The global maxima (represented by circles) and minima (represented by crosses) of the order parameters r_1 (green markers) and r_2 (red markers) are displayed. For values of $\delta < \delta^*$, stationary cyclops states with a constant phase difference within clusters remain stable. Increasing $\delta > \delta^*$ induces switching cyclops states with periodically rearranging clusters as evidenced by the periodicity in the order parameters r_1 and r_2 .

V. CYCLOPS STATES IN NETWORKS OF THETA-NEURONS

Here, we provide evidence that the cyclops state formation mechanism is not limited to Kuramoto networks and is also common in neuronal networks whose dynamics exhibits two time scales and can be approximated by the Kuramoto model with inertia. As a prime example, we consider a network of N identical theta-neurons coupled through a global synaptic drive (see references [57-59] in the main text):

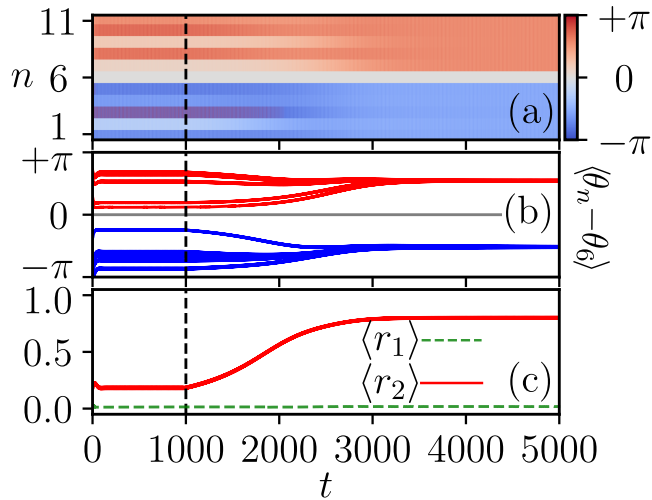
$$\dot{\theta}_n = (1 - \cos \theta_n) + \eta (1 + \cos \theta_n) + \kappa (1 + \cos \theta_n - \varepsilon + \varepsilon \cos 2\theta_n) s(t), \quad (\text{S.13})$$

where $n = 1, \dots, N$ is the index of the n -th neuron whose state is the phase angle θ_n , $\eta > 0$ is an excitability parameter playing the role of a fixed input current. The n th-neuron is set to fire a spike when θ_n crosses π while increasing. The last term on the right-hand side of (S.13) accounts for synaptic interactions. Parameter κ is the coupling strength of the global synaptic drive. The mean population synaptic activity $s(t)$ satisfies the relaxation equation [61]:

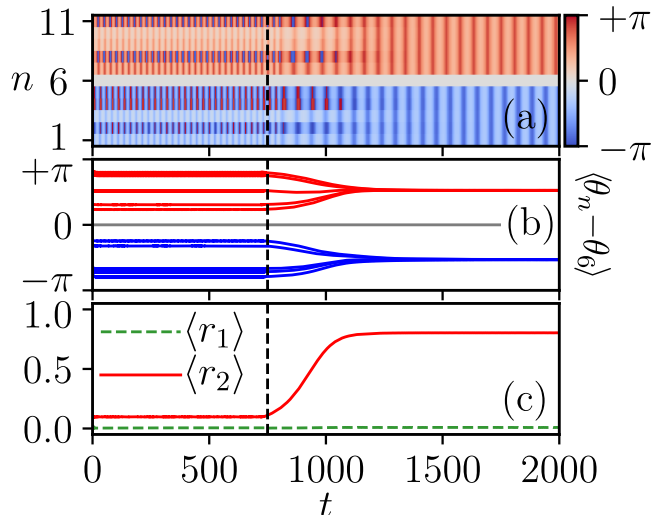
$$\tau \dot{s} = -s + \frac{1}{N} \sum_{n=1}^N P_\ell(\theta_n), \quad (\text{S.14})$$

where the function $P_\ell(\theta_n) = p_\ell (1 - \cos \theta_n)^\ell$ ($\ell \in \mathbb{N}$) determines the sharpness of the pulsatile-type synaptic coupling, and $p_\ell = 2^\ell (\ell!)^2 / (2\ell)!$ is a normalization constant. The positive integer parameter ℓ defines the shape of $P_\ell(\theta_n)$ so that the pulse profile becomes more sharply peaked as ℓ increases, becoming δ -pulses in the limit $\ell \rightarrow \infty$.

Note that the system (S.13) with $\varepsilon = 0$ is the standard theta-neuron model [57-59]. We introduced two additional terms proportional to the small parameter $\varepsilon \ll 1$ to the last term on the right-hand side of (S.13) to take into account neuronal refractoriness [60,61] which results in decreasing the sensitivity of a neuron to stimulus from its pre-synaptic partners in the time interval preceding the spike and for some time after it. In Sec. VII, we will demonstrate how these terms naturally appear from the phase dynamics description of quadratic integrate-and-fire neurons. Notably, one of the additional terms yields the second-order coupling term similar to the Kuramoto network (1). While the effect of neuronal refractoriness in brain networks may be relatively weak, it induces the second-order coupling term similar to the Kuramoto network (1) and can significantly alter the dynamics of the network. Supplementary Figures 6-7 demonstrate that the activation of the second-order harmonics stabilizes a cyclops state, showing the same effect as in the Kuramoto-Sakaguchi network with inertia (1) (see Fig. 4 in the main text).



Supplementary Figure 6: The role of the second harmonics in stabilizing a cyclops state in system (S.13) with $N = 11$, $\eta = 0.3$, $\tau = 0.8$, $\kappa = 0.2$, $\varepsilon = 0.04$, $\ell = 5$. The system with only the first-order coupling ($\varepsilon = 0$) evolves into a generalized splay state with $\langle r_1 \rangle = 0$ from random initial conditions for $0 < t < 750$. Switching on the second harmonics with $\varepsilon = 0.04$ induces a stable cyclops state ($750 < t < 2000$). (a) Colors indicate $\theta_n(t) - \theta_6(t)$. (b) Time-averaged phase differences $\langle \theta_n(t) - \theta_6(t) \rangle$. (c) The corresponding values of $\langle r_1 \rangle$ and $\langle r_2 \rangle$.



Supplementary Figure 7: Stabilization of a cyclops state in system (S.13) as in Supplementary Fig. 6 but for a different set of parameters: $N = 11$, $\eta = 0.5$, $\tau = 0.8$, $\kappa = 1.5$, $\varepsilon = 0.04$, $\ell = 50$. Note the stronger synaptic coupling κ and the breathing cyclops state.

VI. RELATING THE THETA-NEURON NETWORK (S.13) TO NETWORK (1)

The close resemblance between the simulation results of the theta-neuron network and the original Kuramoto-Sakaguchi model of 2D phase oscillators should not be surprising, as the two models are directly related. More specifically, the theta-neuron system (S.13) can be reduced to the original phase model (1). The basic steps of such a reduction are as follows. First, one can use the transformation of dynamical variables given by the relation $\tan(\theta_n/2) = \sqrt{\eta} \tan(\phi_n/2)$. This transformation converts the θ -description of the neuron population into another phase representation. The ϕ -representation is equivalent to the θ -description in that ϕ_n is defined to lie in the interval $[-\pi, \pi]$ and the n -th neuron spikes when ϕ_n passes π . However, in the model (S.13), cells receive constant common external input $\eta > 0$ and all units are in the oscillatory regime. As a result, each phase ϕ_n rotates uniformly in the absence of interaction between the cells, making the ϕ -representation more convenient for further analysis and the derivation of a Kuramoto-type model approximation. Through this process, we obtain the governing equation for the introduced dynamical variables ϕ_n , which coincides with the Winfree model in the fast relaxation limit for the mean

synaptic activity $s(t)$ ($\tau \rightarrow 0$), i.e. in the case of instantaneous coupling [61]. Finally, we assume that the synaptic coupling is weak, allowing us to separate the time scales such that $\phi_n(t)$ can be written as the sum $\phi_n(t) = \vartheta(t) + \varphi_n(t)$ of a fast, free-running rotation with period $\pi/\sqrt{\eta}$ described by $\vartheta(t)$ and slow phase drifts produced by interaction through synaptic stimulus described by the set of slow variables $\varphi_n(t)$. The slow variables $\varphi_n(t)$ can be considered constant over time scales that are comparable to the period of the fast rotation. By applying the method of averaging, we can derive the Kuramoto-Sakaguchi model of 2D phase oscillators from (S.13). It is noteworthy that the resulting pairwise interaction function in the Kuramoto-Sakaguchi model (1) contains both the first-order and second-order harmonics (the latter being proportional to ε). A detailed derivation and technical aspects of the described approach will be presented elsewhere.

VII. DERIVING THE THETA-NEURON NETWORK (S.13) FROM QUADRATIC INTEGRATE-AND-FIRE NEURONS

Here, we demonstrate that the theta-neuron model (S.13) can be derived from a network of quadratic integrate-and-fire (QIF) neurons, implying that cyclops states may also occur in QIF networks. We have not explored cyclops states in QIF networks in this study, but it is an area of future research.

We consider a globally coupled network of N identical QIF neurons ($n = 1, 2, \dots, N$) [61]:

$$\begin{aligned} \dot{v}_n &= v_n^2 + \eta + \kappa j_n(t) & \text{if } v_n < v_{th}, \\ v_n &= v_r & \text{if } v_n \geq v_{th}, \end{aligned} \quad (\text{S.15})$$

where η is an applied constant current, κ is a common synaptic weight controlling the total strength of synaptic inputs, and $j_n(t)$ is a time-varying input drive. When the membrane potential v_n of the n th neuron reaches the threshold value v_{th} , the neuron generates a spike and its voltage is reset to v_r . We consider the limit $v_{th} = -v_r \rightarrow \infty$. In the absence of other inputs ($j_n(t) = 0$), the applied current $\eta = 0$ places the system at a saddle-node bifurcation, responsible for the onset of tonic (periodic) firing.

As discussed above, the sensitivity of a neuron to stimulus from other cells may decrease before and after the spike due to refractoriness. This can be modeled by the following expression for the recurrent input:

$$j_n(t) = F(v_n)s(t), \quad s(t) = \frac{1}{N} \sum_{n=1}^N \sum_{k \setminus t_n^k < t} \int_{-\infty}^t d\tilde{t} G_\tau(t - \tilde{t}) \delta(\tilde{t} - t_n^k). \quad (\text{S.16})$$

Here, $s(t)$ is the mean synaptic activation, t_n^k is the time of k -th spike of the n -th neuron, $\delta(t)$ is the Dirac delta function, and $G_\tau(t)$ is the normalized synaptic activation caused by a single presynaptic spike with time scale τ , e.g., $G_\tau(t) = e^{-t/\tau}/\tau$. The function $F(v_n)$ describes the sensitivity of the n -th neuron to stimulus from its presynaptic partners. We define $F(v_n)$ as

$$F_n(v) = 1 - 4\varepsilon v_n^2 / (1 + v_n^2). \quad (\text{S.17})$$

The transformation $v_n(t) = \tan(\theta_n(t)/2)$ [57] converts the membrane potential description of the QIF model (S.15) into a phase description, leading to the phase equation

$$\dot{\theta}_n = (1 - \cos \theta_n) + \eta(1 + \cos \theta_n) + \kappa(1 + \cos \theta_n)(1 - 2\varepsilon(1 - \cos \theta_n))s(t), \quad (\text{S.18})$$

which coincides with (S.13).